




New FeVTaO₆ compound—synthesis, structure and selected properties

Elżbieta Filipek^{1,*} , Mateusz Piz¹, Grażyna Dąbrowska¹, Piotr Dulian², Małgorzata Karolus³, and Maciej Zubko^{3,4}

¹ Department of Inorganic and Analytical Chemistry, Faculty of Chemical Technology and Engineering, West Pomeranian University of Technology in Szczecin, Al. Piastów 42, 71-065 Szczecin, Poland

² Faculty of Chemical Engineering and Technology, Cracow University of Technology, 24, Warszawska St., 31-155 Kraków, Poland

³ Institute of Materials Engineering, University of Silesia, 75 Pułku Piechoty 1A, 41-500 Chorzów, Poland

⁴ Department of Physics, Faculty of Science, University of Hradec Králové, Rokitsanského 62, 500 03 Hradec Králové, Czech Republic

Received: 28 June 2023

Accepted: 15 November 2023

Published online:
15 December 2023

© The Author(s), 2023

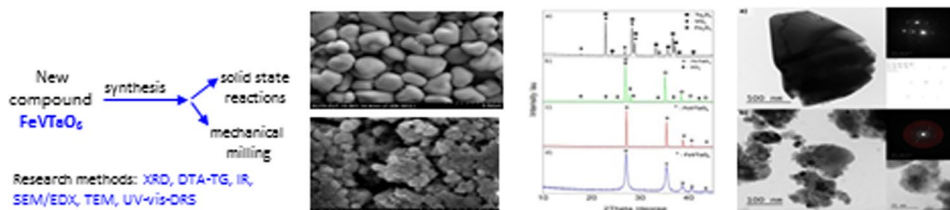
ABSTRACT

A new ceramic compound of the chemical formula FeVTaO₆ was obtained in polycrystalline form, as a result of a high-temperature reaction between Fe₂O₃, Ta₂O₅ and VO₂ mixed at the molar ratio 1:1:2 as well as in the reaction of equimolar mixture of FeTaO₄ with VO₂. The synthesis of this new compound has also been carried out by mechanochemical method realized by high-energy ball milling of some mixture of reactants. FeVTaO₆, in both cases, was obtained under an atmosphere of deoxygenated argon. The new compound was characterized by XRD, DTA-TG, IR, SEM/EDX, TEM, XRF and UV-vis-DRS methods. Using X-ray powder diffraction, the lattice parameters of the unit cell and the parameters of the positioning of atoms (Rietveld analysis) were determined, and grain sizes were obtained on the basis of diffraction line broadening. The results showed that FeVTaO₆ crystallizes in the tetragonal system with rutile-type structure. As shown in the DTA results, regardless of the synthesis method, FeVTaO₆ is stable in argon atmosphere up to ~1225 °C and in air up to ~925 °C. Based on the UV-Vis-DR spectra, it was also established that the obtained compound is a semiconductor. The energy gap value determined for the compound obtained by the solid-state method is E_g ~ 1.75 eV, and for the compound obtained by the mechanochemical method E_g ~ 2.10 eV.

Handling Editor: David Cann.

Address correspondence to E-mail: elafil@zut.edu.pl

GRAPHICAL ABSTRACT



Introduction

The recent development of such industries as chemical, electronic, energy, textile or automotive industries requires the search for new, previously unknown phases that can be components of modern, advanced materials with attractive and competitive in terms of application, physicochemical properties.

Research in the field of materials science often concerns mainly on the modification of already used materials in order to improve their functional properties, a reduced consumption of raw materials and energy by industrial production technologies, as well as limited their negative impact on the environment. Less frequently, such research includes the design and production of new materials, especially advanced ones, with the desired chemical, mechanical, thermal and other properties, in particular, due to their time-consuming and complex nature. Application research is always preceded by comprehensive, continuous basic research, from which we know not only the synthesizing methods of new phases, but also their physicochemical and structural characteristics. Such knowledge is the basis for searching for their functional properties and potential applications.

The literature data show that an interesting group of such new phases are compounds and solid solutions formed, inter alia, in multicomponent oxide systems, especially those containing *d* and *f*-electron metal oxides [1–11].

The choice of the research object analyzed in this study was made on the basis of very limited literature data on the three-component $\text{Fe}_2\text{O}_3\text{--Ta}_2\text{O}_5\text{--VO}_2$ system [12] and the research experience of employees of the Department of Inorganic and Analytical Chemistry of the Faculty of Chemical Technology and Engineering, ZUT [9–11, 13–16].

The most thermodynamically stable forms of oxides, i.e., the hexagonal form $\alpha\text{-Fe}_2\text{O}_3$, low-temperature

$\beta\text{-Ta}_2\text{O}_5$ crystallizing in the orthorhombic structure and the monoclinic vanadium(IV) oxide polymorph [17–19], were used for the syntheses in this work.

The physicochemical properties of these types of oxides and the range of their applications are well known [17–33].

It is known that hexagonal iron(III) oxide, due to its electrical, optical and magnetic properties [20–22], has many applications, including the production of inorganic pigments, gas sensors and electronic devices such as devices for data storage and magnetocaloric cooling, bioprocessing or in the production of ferrofluids and adsorbents for wastewater treatment [23, 24].

Tantalum(V) oxide with an orthorhombic structure due to its high dielectric and refractive index as well as excellent photoelectric parameters [25, 26] is used in the production of photovoltaic, electronic devices, and also as a material for the anti-reflective coatings. Moreover, Ta_2O_5 has several advantages over the other materials like low cost, non-toxicity, availability and structural stability [27–29].

Vanadium dioxide, the third component of the reaction mixtures, is a typical metal–insulator transition material (MIT) that passes from the monoclinic insulating phase (M) at room temperature to the high-temperature rutile metallic phase (R) [30, 31]. The phase transition of VO_2 is accompanied by sudden changes in electrical conductivity and optical transmittance. Due to its specific phase transition characteristics, VO_2 is widely studied for applications in electrical and optical devices, smart windows, sensors, actuators, etc. [32, 33].

In the available literature, no studies of the phases formed in two-component oxide systems, i.e., $\text{Fe}_2\text{O}_3\text{--VO}_2$ and $\text{Ta}_2\text{O}_5\text{--VO}_2$, were found, which are side limitations of the $\text{Fe}_2\text{O}_3\text{--Ta}_2\text{O}_5\text{--VO}_2$ system selected for this study. It is known that in the third of these lateral systems, namely $\text{Fe}_2\text{O}_3\text{--Ta}_2\text{O}_5$, only one compound with the rutile structure is formed,

i.e., FeTaO_4 [34–36]. The methods of synthesis of this compound and its magnetic properties are known [34, 35]. From the few literature data [9] it is also known that in the Fe_2O_3 – Ta_2O_5 – VO_2 system only one phase is formed, the limited solid solution type with the formula $\text{Fe}_x\text{Ta}_x\text{V}_{2-2x}\text{O}_4$ and the homogeneity range for $0.01 \leq x \leq 0.35$. The $\text{Fe}_x\text{Ta}_x\text{V}_{2-2x}\text{O}_4$ phase was obtained by heating FeTaO_4 mixtures with VO_2 in a vacuum, sealed quartz ampoules at a temperature of 1100 °C for 40–50 h [9].

The main goal of this study was to determine the synthesis conditions of the previously unknown FeVTaO_6 compound, formed with the participation of three oxides Fe_2O_3 , Ta_2O_5 and VO_2 , and to study its properties and structure. In addition to the classic high-temperature solid-phase synthesis method, an attempt was made to obtain this new compound by a mechanochemical method that guarantees smaller crystallite sizes, which is important due to its potential use, *inter alia* as a catalyst.

Determining the basic physicochemical properties of FeVTaO_6 will help identify other potential areas of its applications, including in electrical and optical devices or in the process of photocatalytic hydrogen production [23–26, 32, 33, 37].

The latter potential application [37] may be of particular interest, as photocatalytic hydrogen evolution represents a transformative pathway in addressing fossil fuel challenges, heralding a renewable and pristine alternative to conventional fossil fuel-based energy paradigms. A formidable challenge, therefore, is to develop a stable photocatalyst with high efficiency that optimizes solar energy transduction and charge sharing even under adverse conditions.

Experimental procedure

Sample preparation

To synthesize monophase samples contained FeVTaO_6 , the following reagents were used: Fe_2O_3 —a.p. (POCh, Poland), Ta_2O_5 —a.p. (Alfa Aesar, Germany), VO_2 —a.p. (Alfa Aesar, Germany) and separately obtained compound— FeTaO_4 (PDF card—01-071-0932) by method described, for example, in the paper [35].

The high-temperature solid-state reaction

Reagents weighed in suitable proportions were homogenized and calcined in argon atmosphere in the temperature range 700–920 °C in a tube furnace PRC 50/170/M (Czylok, Poland). After each heating stage, the samples were gradually cooled in the furnace to room temperature, weighed (changes in their mass and their color were recorded) and analyzed.

Mechanochemical synthesis

Mechanochemical synthesis (MChS) using laboratory planetary ball mill *Pulverisette-6* (Fritsch GmbH, Germany) with vessel and balls made of zirconium was carried out under the following conditions: rpm = 500, BPR = 1:20, time = 3.0 and 6.0 h under argon atmosphere, the diameter of the milling balls used is 10 mm. The conditions for mechanochemical syntheses were chosen based on the authors' experience in this field and information available in the scientific literature [38–40].

Methods

The obtained samples were tested using the following methods:

- XRD (the diffractometer EMPYREAN II, PANalytical, Netherlands) analysis using $\text{CuK}\alpha$ radiation ($\lambda = 1.5418 \text{ \AA}$) with graphite monochromator. The phases were identified on the basis of XRD characteristics contained in the PDF cards [41]. The powder diffraction pattern of FeVTaO_6 was indexed by means of FullProf [42] and EXPO2014 programs [43].
- The crystallite size determination was done using the PANalytical Software HighScore Plus 4.0 based on the Rietveld Method [44, 45] and the Williamson–Hall theory [46]. The procedure and its assumptions have been published in detail in previous works [47, 48].
- SEM (FE-SEM Hitachi SU-70 microscope, EDS X-ray Microanalysis using NORAN™ System 7 of Thermo Fisher Scientific (UltraDry X-ray detector)).
- EDXRF (Epsilon3 energy-dispersive X-ray fluorescence spectrometer, Malvern Panalytical)
- IR spectroscopy (SPECORD M-80 Carl Zeiss, Jena, Germany). The measurements were taken within

the wave number range of 1100–300 cm^{-1} . The infrared spectra were made by pelleting a sample with KBr in the weight ratio of 1:300.

- DTA–TGA (SDT 2960, TA Instruments, USA) measurements in the temperature range 20–1500 °C in argon atmosphere, mass of samples ~ 20 mg, heating rate 10 deg/min.
- DTA–TGA (SDT 650, TA Instruments, USA) measurements in the temperature range 20–1250 °C in air atmosphere, mass of samples ~ 20 mg, heating rate 10 deg/min.
- UV–Vis–DR spectroscopy (V-670 JASCO, Japan) equipped with a reflecting attachment for the solid-state investigation (integrating sphere attachment with horizontal sample platform PIV-756/(PIN-757). The spectra were recorded in the wavelength region of 200–750 nm at room temperature.
- The density of FeVTaO_6 were determined in argon (5N purity) with the help of an Ultrapyc 1200e ultracycrometer (Quantachrome Instruments, USA).
- The transmission electron microscopy (TEM) observations were performed using a JEOL high-resolution (HRTEM) JEM 3010 microscope operating at a 300 kV accelerating voltage, equipped with a Gatan 2 k × 2 k Orius™ 833SC200D CCD camera. The powder samples were suspended in isopropanol and the resulting material after dispersion in ultrasonic bath was deposited on a Cu grid with an amorphous carbon film standardized for TEM observations. Selected area electron diffraction (SEAD) patterns were indexed using dedicated EIDyf software.

Results and discussion

Synthesis and properties of the FeVTaO_6 compound

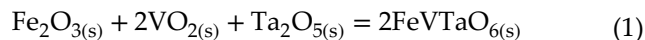
The synthesis of FeVTaO_6 was carried out using two different methods: high-temperature solid-phase reactions and mechanochemical synthesis.

The synthesis of FeVTaO_6 by the “high-temperature solid-phase” method was carried out in an argon atmosphere using the following starting reagents: a mixture of oxides composed of 25.00 mol% Fe_2O_3 , 50.00 mol% VO_2 and 25.00 mol% Ta_2O_5 and a mixture of 50.00 mol% VO_2 and 50.00 mol% FeTaO_4 .

After homogenization and pelletization, mixtures of appropriate reagents were heated, under

argon, in the following stages: 700 °C (12 h) → 800 °C (12 h) → 900 °C (12 h) → 925 °C (12 h).

The results of the X-ray phase analysis of the samples after the last stage of their heating showed that, regardless of the type of reactants contained in the reaction mixtures, as a result of reactions taking place in the solid phase, a new compound with the formula FeVTaO_6 is formed, according to the following reaction equations:



The mechanochemical method was also used to obtain FeVTaO_6 compound after two 3-h steps of grinding the mixture of substrates with the composition of 50.00 mol% VO_2 and 50.00 mol% FeTaO_4 (reaction 2), under argon atmosphere.

FeVTaO_6 has a graphite color. Figure 1 shows, next to fragments of XRD patterns of starting mixtures (Fig. 1a, b), a fragment of a diffractogram of FeVTaO_6 compound obtained by high-temperature synthesis (Fig. 1c) and the mechanochemical method (Fig. 1d).

In Fig. 1, the diffraction patterns of initial mixtures (Fig. 1a and b) and diffractograms of final products obtained by the high-temperature reaction method (WT) (Fig. 1c) and mechanical synthesis (MCS) (Fig. 1d) are presented. The diffraction lines on the diffraction pattern of FeVTaO_6 obtained by the mechanochemical method (Fig. 1d) are very broad compared to the analogous ones recorded for this compound obtained by high-temperature solid-state synthesis (Fig. 1c). This result indicates that the size of the crystallites of the FeVTaO_6 compound obtained by the mechanochemical method leads to formation of nanocrystalline phases. In order to confirm this fact, an analysis of the diffraction profiles using the Williamson–Hall method was performed. The obtained results showed that values of crystallite size and lattice strain of FeVTaO_6 obtained by high-temperature reaction method are: ~ 1000 Å and 0.10%, respectively, and obtained by the mechanochemical method are 151 Å and 1.08%, respectively. It is worth pointing out that in the case of both methods, the same phase is formed, which is clearly visible in Fig. 2.

Indexing of the powder diffraction pattern of FeVTaO_6 was performed using the FullProf and EXPO2014 programs [42, 43]. 25 successive diffraction lines registered in the angular range

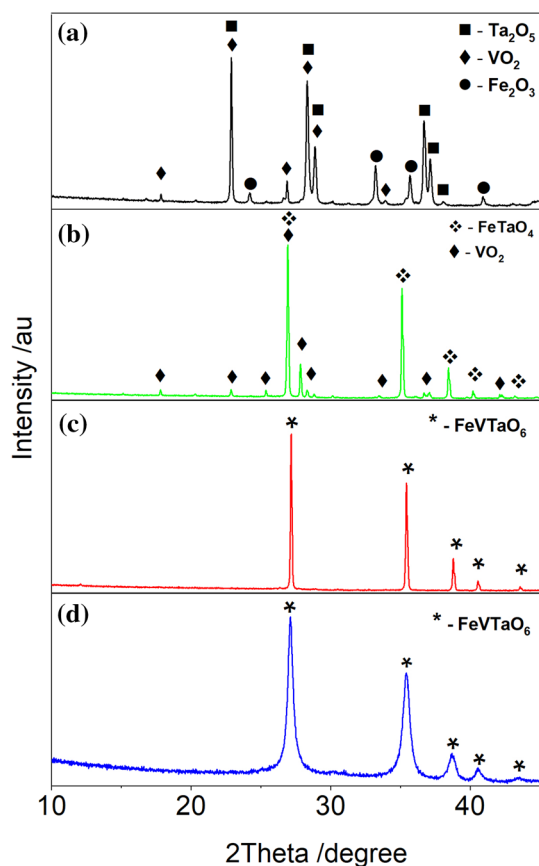
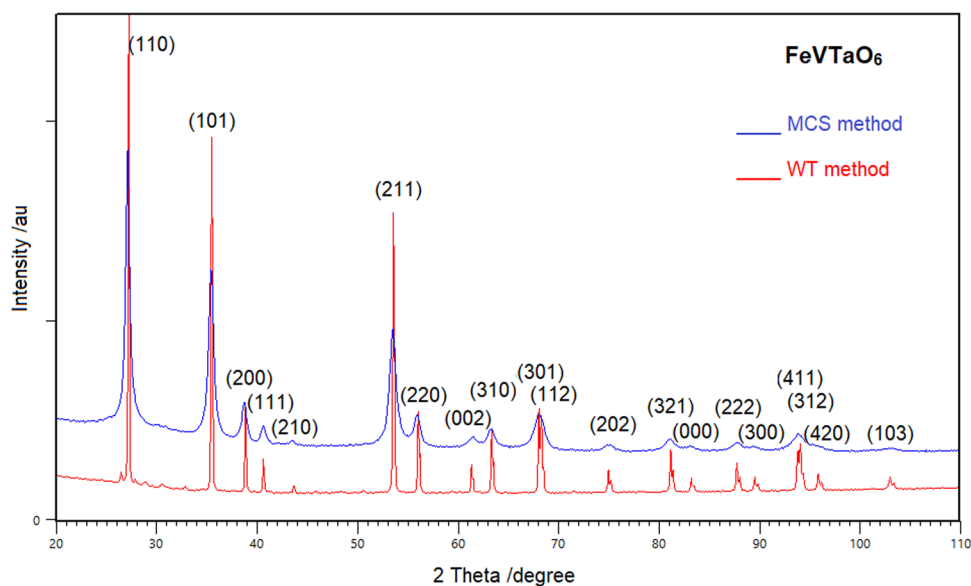


Figure 1 Fragments of XRD patterns **a** a starting mixture with the composition of 25.00 mol% Fe_2O_3 , 50.00 mol% VO_2 and 25.00 mol% Ta_2O_5 , **b** the initial mixture composed of 50.00 mol% VO_2 and 50.00 mol% FeTaO_4 , **c** FeVTaO_6 obtained by the method of high-temperature reactions, **d** FeVTaO_6 obtained by a mechanochemical method

Figure 2 Comparison of diffraction patterns of FeVTaO_6 obtained by the high-temperature reaction method (WT—red line) and by the mechanochemical method (MCS—blue line). Miller indices obtained from EXPO analysis (Table 1)



10–130° 2θ ($\text{CuK}\alpha$) were subjected to indexing. When choosing solution, high values of the “figure of merit” $F(25) = 24(0.021507)$ were taken into account.

Based on the collected powder diffraction patterns for the FeVTaO_6 compound after mechanochemical synthesis the full Rietveld refinement was performed using FullProf program suite. The fitting results can be seen in Fig. 3.

The Rietveld refinement results for the studied compound are given in Table 1.

The studied structure crystallizes in tetragonal crystal system in the $P4_2/mnm$ space group (group number 136). Metal atoms are located on 2a special Wyckoff position, whereas oxygen atom is located on 4f special Wyckoff position what indicate that only the oxygen atom $x = y$ coordinates can be refined (obtained value from the refinement is 0.2978(5)). The theoretical density of the compound FeVTaO_6 has been calculated and is 652 g/cm^3 .

Scanning electron microscope (SEM)

In the next stage of the research, the FeVTaO_6 compound was examined by scanning electron microscopy. Figure 4a shows the image of the crystals of the compound obtained by the solid-state method, and in Fig. 4b, the mechanochemical method.

Figure 4a and b shows significant differences in the crystal morphology. The crystals of the FeVTaO_6 compound obtained by solid-state synthesis have the shape of irregular polyhedra and the size of $\sim 2 \mu\text{m}$, while the crystals of the compound obtained

Figure 3 Result of the Rietveld refinement of the FeVTaO₆ sample obtained by the mechanochemical method. Red circles represent experimental points, black solid line represents calculated profile, blue solid line shows the difference curve whereas the green vertical lines indicate the Bragg positions. Inset shows image of the resulting crystal structure—metal atoms are shown as the grayish ball inside green octahedra with oxygen atoms on the corners shown as red balls

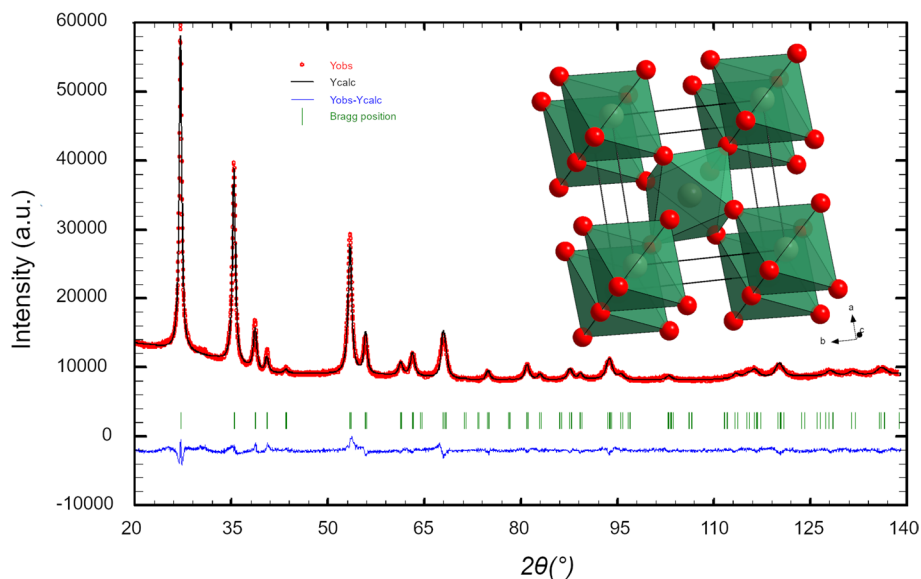
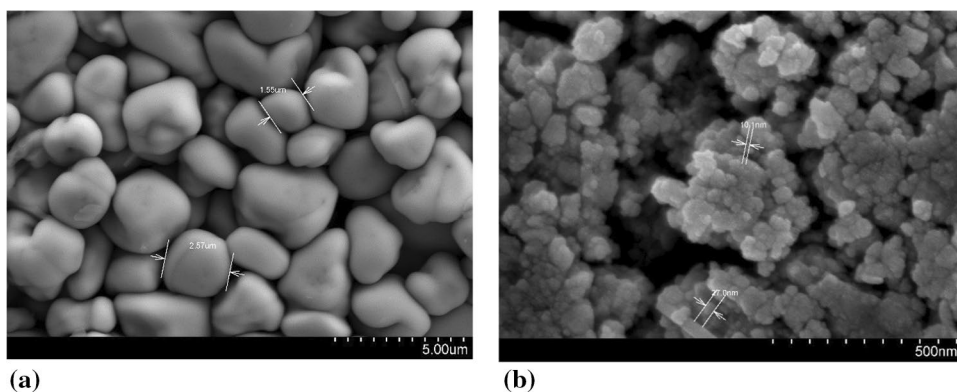


Table 1 Results of the Rietveld refinement for the studied compound

Formula (Z=2)		FeTaVO ₆					
$a=b$ (Å)	4.6546 (1)	V (Å ³)	65.51 (1)				
c (Å)	3.0236 (1)	Space group	$P4_2/mnm$				
Scale factor	0.0823 (3)						
Zero point	-0.037 (5)						
$2\theta_{\min} = 19^\circ$	$2\theta_{\max} = 140^\circ$	$2\theta_{\text{step}} = 0.026^\circ$	No. points = 4654				
λ_1/λ_2 (Å)	1.54059/1.54431	No. refined para	30				
R_{wp}	0.1110	R_p	0.1510				
R_{Bragg}	0.0353	R_F	0.0337				
R_{exp}	0.0482	χ^2	5.26				
Atom	x	y	z	B	occ	Site	
Fe	0.0000	0.0000	0.0000	1.07 (2)	0.333	2a	
Ta	0.0000	0.0000	0.0000	1.07 (2)	0.333	2a	
V	0.0000	0.0000	0.0000	1.07 (2)	0.333	2a	
O	0.2978 (5)	0.2978 (5)	0.0000	1.30 (10)	1.0	4f	

Figure 4 SEM image of FeVTaO₆ crystals obtained by the method **a** high-temperature solid-state reactions, **b** mechanochemical method



mechanochemically have the shape of fine plates with sizes ~ 20 nm.

The X-ray microanalysis of the content of metallic elements in the tested samples was performed at several points, selecting crystals for testing, one of the faces of which was perpendicular to the electron beam. Analysis showed the presence of iron, vanadium and tantalum in the following averaged amounts:

- For FeVTaO_6 obtained in solid-state method: Fe—22.15 mass%, V—14.6 mass% and Ta—63.53 mass%,
- For FeVTaO_6 obtained mechanically: Fe—19.70 mass %, V—17.63 mass% and
- Ta—62.45 mass%, in relation to the calculated from the formula Fe—19.41 mass%,
- V—17.70 mass% and Ta—62.89 mass%.
- Chemical composition of the obtained compound was determined also with XRF method and was as follows:
- For FeVTaO_6 obtained in solid-state method: Fe—19.46 mass%, V—14.99 mass% and Ta—65.55 mass%,
- For FeVTaO_6 obtained mechanically: Fe—20.20 mass%, V—15.85 mass% and Ta—63.95 mass%.

The correctness of the proposed formula is indicated by Rietveld analysis, as well as by the composition of the substrate mixtures used in the reaction, which corresponds to the stoichiometry of the FeVTaO_6 compound, and the course of the reaction without a significant change in mass.

As part of the work, the density of FeVTaO_6 compound was determined using an ultrapikeometer, which is: $\sim 6.18 \text{ g/cm}^3$ (mechanochemical synthesis) and $\sim 6.51 \text{ g/cm}^3$ (synthesis by high-temperature reactions).

Transmission electron microscopy (TEM)

Performed TEM observations confirmed the results obtained by the X-ray diffraction analysis. Vast differences in the samples morphology can be observed (Fig. 5). Sample after high-temperature solid-state reactions is composed mostly of the large crystallites whereas sample obtained by a mechanochemical method is composed of nanosized crystallites. Performed manual image analysis indicated that after measuring 198 particles the average size is 36 nm with standard deviation of 25 nm. Such high standard

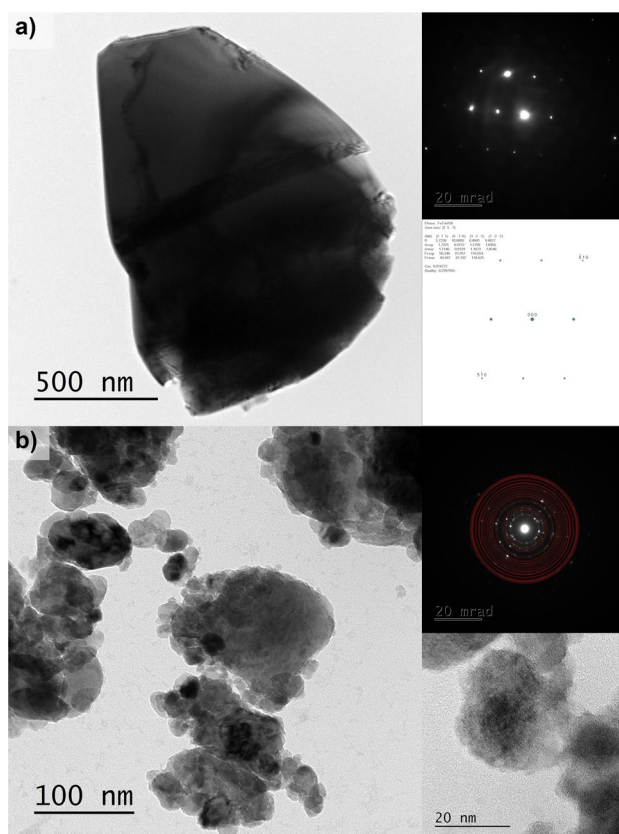


Figure 5 Bright field TEM images of the FeVTaO_6 after **a** high-temperature solid-state reactions and **b** obtained by a mechanochemical method. Right part of the figure shows selected area electron diffraction patterns collected from the observed regions. Red ring indicates theoretical rings corresponding to the FeVTaO_6

deviation indicates the broad distribution of the particles size, what can be seen of Fig. 6.

The particles size distribution follows closely the LogNormal distribution as can be expected. The recorded selected area electron diffraction (SAED) patterns are in good agreement to the FeVTaO_6 phase for both studied samples: after high-temperature solid-state reactions and obtained by a mechanochemical method.

Thermal analysis (DTA-TG)

In the next stage of work, the FeVTaO_6 compound was tested by differential thermal analysis combined with thermogravimetry up to 1500 °C in an argon atmosphere. In the DTA curve of the FeVTaO_6 compound, presented in Fig. 7, one endothermic effect with the onset temperature equal to 1225 °C was recorded.

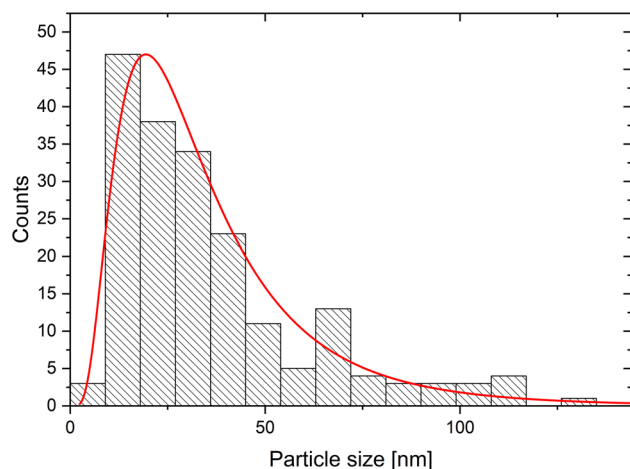


Figure 6 Particles size distribution of the FeVTaO₆ sample obtained by a mechanochemical method

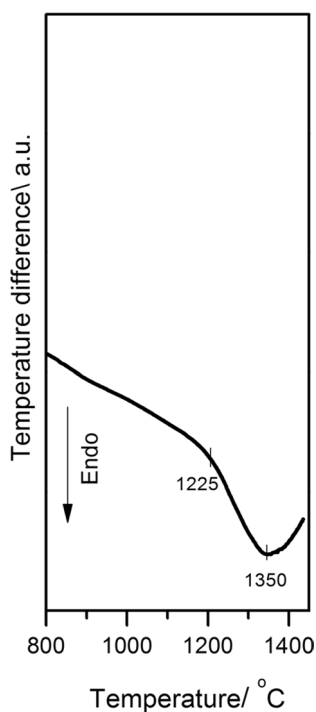


Figure 7 DTA curve of the FeVTaO₆ compound

It was also found that the sample after this test was molten, which means that the compound FeVTaO₆ melts under an argon atmosphere at a temperature of 1225 °C.

Phase analysis (XRD) of the sample after DTA-TG examination revealed mainly the presence of tetragonal FeTaO₄ (PDF no 01-071-0932) as a solid melting product of FeVTaO₆ in argon.

In order to determine the thermal stability of FeVTaO₆ in air, this compound was subjected to DTA-TG tests in such an atmosphere, but due to technical limitations only up to the temperature of 1250 °C. No significant thermal effect was recorded on the DTA curve, but on the TG curve, the weight loss of the sample started as early as 925 °C.

To determine the melting or decomposition products of FeVTaO₆ in air, a sample containing only this compound was heated in a muffle furnace at 925 °C for 3 h and then rapidly cooled to ambient temperature. X-ray phase analysis of the sample melted under these conditions showed the presence of FeTaO₄ compound and V₂O₅ oxide. Vanadium(V) oxide no longer exists as a solid phase at a temperature of 925 °C, so it seems to be one of the phases crystallizing from a liquid. An additional confirmation of this fact is that the diffraction lines characterizing this oxide were shifted toward lower angles, and the mutual relations of their intensity significantly differed from the intensities reported in the literature [49].

At this stage of the research, it cannot be ruled out that in the air atmosphere the compound initially decomposes into FeTaO₄ and VO₂ oxide, and then vanadium(IV) oxide is oxidized with oxygen from the air to V₂O₅, which is crystallizes from the liquid after melting.

Regardless of the melting /decomposition mechanism, the DTA-TG studies undoubtedly allowed to state that FeVTaO₆ is stable in the air atmosphere up to the temperature of 925 °C, and in the argon atmosphere up to the temperature of 1225 °C.

This temperature difference (~ 300 °C) is due to the reaction with oxygen in the air, one of the decomposition products, i.e., VO₂ to V₂O₅.

Uv-vis-DR spectroscopy

The Uv-Vis-DR spectroscopy method was used to determine the energy gap of the obtained compound, FeVTaO₆. For this purpose, the UV-vis-DR spectra of the compound obtained both by solid-state synthesis and mechanochemically were recorded and then transformed using the Kubelka–Munk function according to the following relationship [50]:

$$F(R) = (1 - R)^2 / 2R \quad (3)$$

where R is reflectance. The value of the energy gap E_g and the absorption coefficient α are related to the following relationship [50, 51]:

$$F(R) \times hn = a \times hn = A(hn - E_g)^2 \quad (4)$$

where: A —constant characterizing a given material, h —Planck's constant, ν —light frequency.

The value of the energy gap of the analyzed solutions was determined from the intersection with the axis of the tangential energy led to the linear segment of the relationship $(\alpha \cdot h\nu)^2$ (Fig. 8).

FeVTaO_6 has been found to be a semiconductor. The value of the energy gap determined for the compound obtained by solid-state synthesis is $E_g \sim 1.75$ eV, and obtained by the mechanochemical method $E_g \sim 2.10$ eV. The obtained results are consistent with the literature data, which show that with

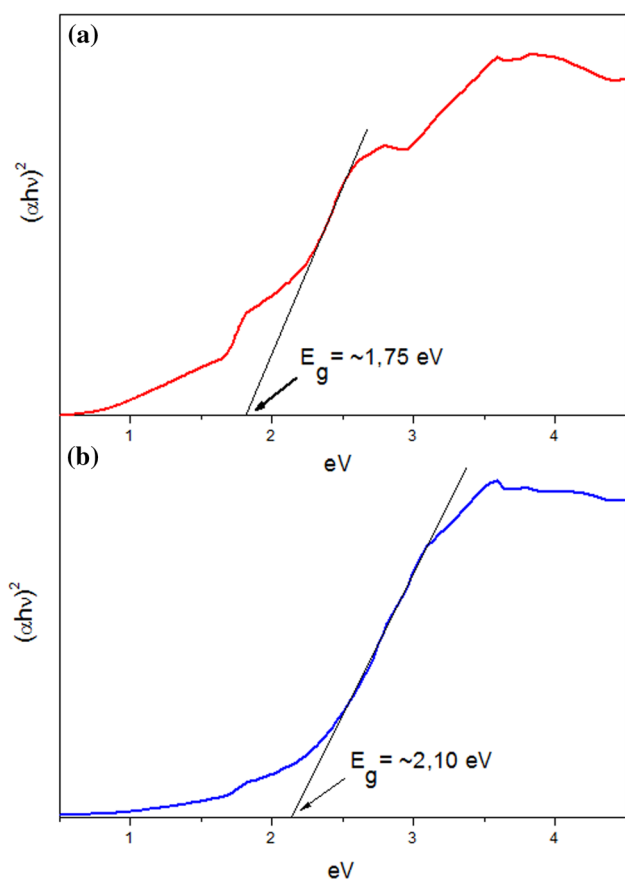


Figure 8 The relationship $(\alpha h\nu)^2$ as a function of the photon energy $h\nu$ with the determined value of the energy gap E_g for **a** FeVTaO_6 compound obtained in the solid-state reaction, **b** compound FeVTaO_6 obtained mechanochemically

the increase in the size of the crystallites, the value of the energy gap decreases [52].

IR spectroscopy

Figure 8 presents an IR spectrum of a mixture of oxides comprising 25.00 mol% Fe_2O_3 , 25.00 mol% Ta_2O_5 and 50.00 mol% VO_2 (a) next to an IR spectrum of the compound obtained from this mixture, i.e., FeVTaO_6 by the mechanochemical method (b) and by solid-state reaction (c).

Figure 9 indicates that the IR spectrum of the compound differs from the spectrum of the oxides mixture both as to the number of the registered bands, their location and as to their intensities. In accordance with the literature data, absorption bands comprising the IR spectrum of the oxides mixture (Fig. 9a) correspond to the stretching or deformation vibrations of the bonds in the coordinating polyhedra in the structure of these oxides [53–57].

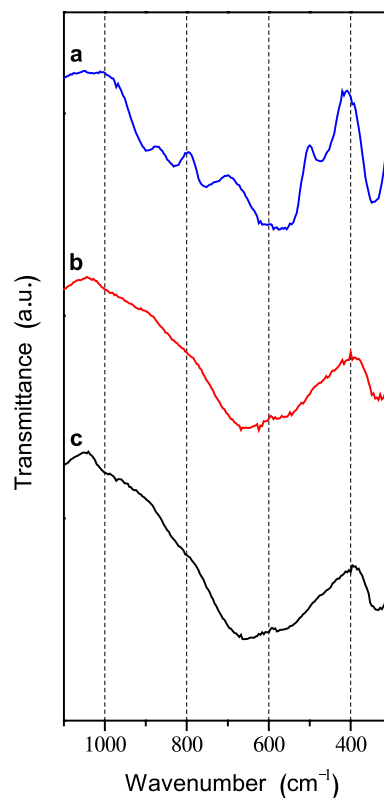


Figure 9 IR spectrum of **a** a mixture of oxides comprising 25.00 mol% Fe_2O_3 , 25.00 mol% Ta_2O_5 and 50.00 mol% VO_2 **b** FeVTaO_6 obtained by the mechanochemical method **c** FeVTaO_6 obtained by solid-state reaction

Absorption bands characteristic for the FeVTaO_6 phase were recorded within the wave-number range $1100\text{--}3000\text{ cm}^{-1}$. Unlike the IR spectrum of the oxides mixture, the spectrum of FeVTaO_6 possesses two absorption band. As follows from peruse of the literature, these bands are characteristic of solid tantalanes(V), antimonates(V) and vanadates(V) with a rutile and trirutile type structure [58–60]. The first broad absorption band is recorded within the range of wave numbers $850\text{--}400\text{ cm}^{-1}$, with the maximum at 650 cm^{-1} . This band can be ascribed to stretching vibrations of the bonds Fe–O in FeO_6 octahedra [61–63] as well as to stretching vibrations of the bonds Ta–O in TaO_6 octahedra [64, 65]. The position of the absorption band of maximum at 330 cm^{-1} in the vibration spectrum of FeVTaO_6 implies that it can be assigned to the deformation vibrations of the O–M–O bond (O–Fe–O, O–V–O, O–Ta–O) and V–O bonds in the distorted MO_6 octahedra or it has a mixed character [66–68].

The IR spectrum of FeVTaO_6 , a phase whose structure has not previously been known, implies that it is built from MO_6 (where M = V, Fe, Ta) octahedra and adopt rutile type structure.

Conclusions

As part of the research, a new, previously unknown compound FeVTaO_6 were obtained as a result of the reaction of the substrate mixture containing 50.00 mol% VO_2 and 50.00 mol% FeTaO_4 , in an argon atmosphere by two different methods, i.e., the high-temperature solid-state method and the mechanochemical synthesis. The compound was also obtained by the high-temperature method by reacting a mixture of oxides; 25.00 mol% Fe_2O_3 , 50.00 mol% VO_2 and 25.00 mol% Ta_2O_5 , under argon. The new compound crystallizes in the tetragonal system and in the P4/mmm space group. The IR spectrum of FeVTaO_6 suggests that the compound is composed of MO_6 octahedrons (where M = V, Fe, Ta) and has a rutile-type structure.

FeVTaO_6 is stable in the air atmosphere up to the temperature of $925\text{ }^\circ\text{C}$, and in the argon atmosphere up to the temperature of $1225\text{ }^\circ\text{C}$. FeVTaO_6 is a semiconductor. The energy gap value of the compound obtained by the solid-state method is $E_g \sim 1.75\text{ eV}$, and for the compound obtained by mechanochemical method $E_g \sim 2.10\text{ eV}$.

Acknowledgements

Not applicable.

Data availability

Not applicable.

Declarations

Conflict of interest The authors declare that they have no known competing financial interests or personal relationships that could have appeared to influence the work reported in this paper.

Ethical approval This study and included experiments have no ethical issues involved.

Open Access This article is licensed under a Creative Commons Attribution 4.0 International License, which permits use, sharing, adaptation, distribution and reproduction in any medium or format, as long as you give appropriate credit to the original author(s) and the source, provide a link to the Creative Commons licence, and indicate if changes were made. The images or other third party material in this article are included in the article's Creative Commons licence, unless indicated otherwise in a credit line to the material. If material is not included in the article's Creative Commons licence and your intended use is not permitted by statutory regulation or exceeds the permitted use, you will need to obtain permission directly from the copyright holder. To view a copy of this licence, visit <http://creativecommons.org/licenses/by/4.0/>.

References

- [1] Isasi J, Veiga ML, Pico C (1996) Synthesis and magnetic and electrical properties of new ternary chromium oxides with the rutile structure. *J Mater Sci Lett* 15:1022–1024. <https://doi.org/10.1007/BF00274894>
- [2] Srivastava JK, Muralidhara Rao S (1978) Search for reclusing of Fe^{3+} ions in the incompletely annealed $\text{Cr}_2\text{O}_3\text{--Fe}_2\text{O}_3$ solid solutions. *Phys Status Solidi (b)* 90:175–177. <https://doi.org/10.1002/pssb.2220900253>

- [3] Govorov VA, Abakumov AM, Rozova MG et al (2005) $\text{Sn}_{2-2x}\text{Sb}_x\text{Fe}_x\text{O}_4$ Solid solutions as possible inert anode materials in aluminum electrolysis. *Chem Mater* 17:3004–3011. <https://doi.org/10.1021/cm048145i>
- [4] Martinelli A, Ferretti M, Basso R, Cabella R, Lucchetti G (2006) Solid state solubility between SnO_2 and $(\text{FeSb})\text{O}_4$ at high temperature. *Z Kristallogr* 221:716–721. <https://doi.org/10.1524/zkri.2006.221.11.716>
- [5] Pargoletti E, Verga S, Chiarello GL, Longhi M, Cerrato G, Giordana A, Cappelletti G (2020) Exploring $\text{Sn}_x\text{Ti}_{1-x}\text{O}_2$ solid solutions grown onto graphene oxide (GO) as selective toluene gas sensors. *Nanomaterials* 10:761. <https://doi.org/10.3390/nano10040761>
- [6] Grigoryan R, Grigoryan L (2012) Electrophysical properties of solid solutions of $\text{Zn}_{2-x}(\text{Ti}_a\text{Zr}_b)_{1-x}\text{Fe}_{2x}\text{O}_4$. *Open J Inorg Chem* 2:88–92. <https://doi.org/10.4236/ojic.2012.24013>
- [7] Cimino A, Stone FS (2002) Oxide solid solutions as catalysts. *Adv Catal* 47:141–306. [https://doi.org/10.1016/S0360-0564\(02\)47007-1](https://doi.org/10.1016/S0360-0564(02)47007-1)
- [8] Kumada N, Nakanome K, Yanagida S, Takei T, Fujii I, Wada S, Moriyoshi Ch, Kuroiwa Y (2018) Crystal structure, photocatalytic and dielectric property of ATiM_2O_8 (A: Mg, Zn; M: Nb, Ta). *J Asian Ceram Soc* 6:247–253. <https://doi.org/10.1080/21870764.2018.1504708>
- [9] Dąbrowska G, Filipek E, Piz M (2015) A new ceramic continuous solid solution in the CrSnSbO_6 – FeSnSbO_6 system and some of its properties. *Ceram Int* 41:12560–12567. <https://doi.org/10.1016/j.ceramint.2015.06.071>
- [10] Błońska-Tabero A, Bosacka M, Filipek E, Piz M, Kochmański P (2020) High-temperature synthesis and unknown properties of $\text{M}_3\text{Cr}_4(\text{PO}_4)_6$ where M = Zn or Mg and a new solid solution $\text{Zn}_{1.5}\text{Mg}_{1.5}\text{Cr}_4(\text{PO}_4)_6$. *J Therm Anal Calorim* 140:2625–2631. <https://doi.org/10.1007/s10973-019-09019-5>
- [11] Tomaszewicz E, Dąbrowska G, Filipek E, Fuks H, Typek J (2016) New scheelite-type $\text{Cd}_{1-3x}\text{Gd}_{2x}(\text{MoO}_4)_{1-3x}(\text{WO}_4)_{3x}$ ceramics—their structure, thermal and magnetic properties. *Ceram Int* 42:6673–6681. <https://doi.org/10.1016/j.ceramint.2016.01.024>
- [12] Kapustkin VK, Fotiev AA, Zolotukhina LV, Pletnev RN (1977) Complex solid solutions $\text{Fe}_x\text{Nb}_x\text{V}_{2-2x}\text{O}_4$ and $\text{Fe}_x\text{Ta}_x\text{V}_{2-2x}\text{O}_4$. *Inorg Mater* 13:2065–2069
- [13] Filipek E, Dąbrowska G, Piz M (2010) Synthesis and characterization of new compound in the V–Fe–Sb–O system. *J Alloys Compd* 490:93–97. <https://doi.org/10.1016/j.jallcom.2009.10.123>
- [14] Piz M, Dulian P, Filipek E, Wiczorek-Ciurowa K, Kochmański P (2018) Characterization of phases in the V_2O_5 – Yb_2O_3 system obtained by high-energy ball milling and high-temperature treatment. *J Mater Sci* 53:13491–13500. <https://doi.org/10.1007/s10853-018-2449-3>
- [15] Filipek E, Piz M (2016) A new compound in the Nb–V–Sb–O system and its physicochemical characteristic. *J Alloys Compd* 661:141–147. <https://doi.org/10.1016/j.jallcom.2015.11.061>
- [16] Dąbrowska G, Filipek E, Tabero P (2022) New solid solution and phase equilibria in the subsolidus area of the three-component CuO – V_2O_5 – Ta_2O_5 oxide system. *Materials* 15:232. <https://doi.org/10.3390/ma15010232>
- [17] Hill AH, Jiao F, Bruce PG, Harrison A, Kockelmann W, Ritter C (2008) Neutron diffraction study of mesoporous and bulk hematite, α - Fe_2O_3 . *Chem Mater* 20:4891–4899. <https://doi.org/10.1021/cm800009s>
- [18] Stephenson NC, Roth RS (1971) Structural systematics in the binary system Ta_2O_5 – WO_3 . V. The structure of the low-temperature form of tantalum oxide L- Ta_2O_5 . *Acta Crystallog B* 27:1037–1044. <https://doi.org/10.1107/S056774087100342X>
- [19] Rogers K (1993) An X-ray diffraction study of semiconductor and metallic vanadium dioxide. *Powder Diffr* 8:240–244. <https://doi.org/10.1017/S0885715600019448>
- [20] Cornell RM, Schwertmann U (2003) The iron oxides: structure, properties, reactions, occurrence and uses. Wiley, Weinheim
- [21] Zboril R, Mashlan M, Petridis D (2002) Iron(III) oxides from thermal processes—synthesis, structural and magnetic properties, mössbauer spectroscopy characterization and applications. *Chem Mater* 14:969–982. <https://doi.org/10.1021/cm0111074>
- [22] Mohapatra M, Anand S (2010) Synthesis and applications of nano-structured iron oxides/hydroxides—a review. *Int J Eng Sci Technol* 2:127–146. <https://doi.org/10.4314/ijest.v2i8.63846>
- [23] Xu H, Wang X, Zhang L (2008) Selective preparation of nanorods and micro-octahedrons of Fe_2O_3 and their catalytic performances for thermal decomposition of ammonium perchlorate. *Powder Technol* 185:176–180. <https://doi.org/10.1016/j.powtec.2007.10.011>
- [24] Gregor C, Hermanek M, Jancik D, Pechousek J, Filip J, Hrbac J, Zboril R (2010) The effect of surface area and crystal structure on the catalytic efficiency of iron(III) oxide nanoparticles in hydrogen peroxide decomposition. *Eur J Inorg Chem* 16:2343–2351. <https://doi.org/10.1002/ejic.200901066>
- [25] Ezhilvalavan S, Tseng TY (1999) Preparation and properties of tantalum pentoxide (Ta_2O_5) thin films for ultra large scale integrated circuits (ULSIs) application—a review. *J*

- Mater Sci 10:9–31. <https://doi.org/10.1023/A:1008970922635>
- [26] Kosiel K, Pałowska K, Kozubal M, Guźwicz M et al (2018) Compositional, structural, and optical properties of atomic layer deposited tantalum oxide for optical fiber sensor overlays. *J Vac Sci Technol* 36:031505. <https://doi.org/10.1116/1.5017725>
- [27] Bright TJ, Watjen JI, Zhang ZM, Muratore C, Voevodin AA, Koukis DI, Tanner DB, Arenas DJ (2013) Infrared optical properties of amorphous and nanocrystalline Ta₂O₅ thin films. *J Appl Phys* 114:083515. <https://doi.org/10.1063/1.4819325>
- [28] Zhu G, Lin T, Cu H, Zhao W, Zhang H, Huang F (2016) Gray Ta₂O₅ nanowires with greatly enhanced photocatalytic performance. *ACS Appl Mater Interfaces* 8:122–127. <https://doi.org/10.1021/acsami.5b07685>
- [29] Nagaraju G, Karthik K, Shashank M (2019) Ultrasound-assisted Ta₂O₅ nanoparticles and their photocatalytic and biological applications. *Microchem J* 147:749–754. <https://doi.org/10.1016/j.microc.2019.03.094>
- [30] Shen N, Dong B, Cao C, Chen Z, Luo H, Gao Y (2015) Solid-state-reaction synthesis of VO₂ nanoparticles with low phase transition temperature, enhanced chemical stability and excellent thermochromic properties. *RSC Adv* 5:108015–108022. <https://doi.org/10.1039/c5ra20732k>
- [31] Zylbersztejn A (1975) Metal-insulator transition in vanadium dioxide. *Phys Rev B* 11:4383–4395. <https://doi.org/10.1103/PhysRevB.11.4383>
- [32] Shen N, Chen S, Huang R, Huang J, Li J, Shi R, Niu S, Amini A, Cheng Ch (2021) Vanadium dioxide for thermochromic smart windows in ambient conditions. *Mater Today Energy* 21:100827. <https://doi.org/10.1016/j.mtener.2021.100827>
- [33] Zhang Y, Xiong W, Chen W, Zheng Y (2021) Recent progress on vanadium dioxide nanostructures and devices: fabrication, properties, applications and perspectives. *Nanomaterials (Basel)* 11:338. <https://doi.org/10.3390/nano11020338>
- [34] Astrov DN, Kryukova NA, Zorin RB, Makarov VA, Ozerov RP, Rozhdestvenskii F, Smirnov VP, Turchaninov AM, Fadeeva NV (1973) Atomic and molecular ordering in MeTaO₄ (Me=Ti, V, Cr, Fe) with rutile structure. *Sov Phys Crystallogr* 17:1017–1023
- [35] Christensen AN, Johanssen T, Lebech B (1976) Magnetic properties and structure of chromium niobium oxide and iron tantalum oxide. *J Phys C: Solid State Phys* 9:2601. <https://doi.org/10.1088/0022-3719/9/13/019>
- [36] Mani R, Achary SN, Chakraborty KR, Deshpande SK, Joy JE, Nag A, Gopalakrishnan J, Tyagi AK (2010) Dielectric properties of some MM'O₄ and MTiM'O₆ (M=Cr, Fe, Ga; M'=Nb, Ta, Sb) rutile-type oxides. *J Solid State Chem* 183:1380–1387. <https://doi.org/10.1016/j.jssc.2010.04.022>
- [37] Yang X, Roy A, Alhabradi M, Alruwaili M, Chang H, Tahir AA (2023) Fabrication and characterization of tantalum-iron composites for photocatalytic hydrogen evolution. *Nanomaterials* 13:2464. <https://doi.org/10.3390/nano13172464>
- [38] Piz M, Dulian P, Filipek E, Wiczcerek-Ciurowa K, Kochmanski P (2018) Characterization of phases in the V₂O₅–Yb₂O₃ system obtained by high-energy ball milling and high temperature treatment. *J Mater Sci* 53:13491–13500. <https://doi.org/10.1007/s10853-018-2449-3>
- [39] Sriram B, Baby JN, Hsu Y, Wang S, George M (2023) Scheelite-type rare earth vanadates TVO4 (T = Ho, Y, Dy) electrocatalysts: Investigation and comparison of T site variations towards bifunctional electrochemical sensing application. *Chem Eng J* 451:138694. <https://doi.org/10.1016/j.cej.2022.138694>
- [40] Tojo T, Zhang Q, Saito F (2007) Mechanochemical synthesis of rare earth orthovanadates from R₂O₃ (R = rare earth elements) and V₂O₅ powders. *J Alloys Compd* 427:219–222. <https://doi.org/10.1016/j.jallcom.2006.02.052>
- [41] Powder diffraction file, international center for diffraction data, Swarthmore (USA). 2022. (PDF-4 +)
- [42] Rodrigez-Carvajal J (1993) Recent advances in magnetic structure determination by neutron powder diffraction. *Phys B: Condens Matter* 192:55–69. [https://doi.org/10.1016/0921-4526\(93\)90108-I](https://doi.org/10.1016/0921-4526(93)90108-I)
- [43] Altomare A, Cuocci C, Giacovazzo C, Moliterni A, Rizzini R, Corriero N, Falcicchio A (2013) EXPO2013: a kit of tools for phasing crystal structures from powder data. *J Appl Crystallogr* 46:1231–1235. <https://doi.org/10.1107/S0021889813013113>
- [44] Young RA (1993) The rietveld method. University Press, Oxford
- [45] McCusker LB, Von Dreele RB, Cox DE, Louër D, Scardi P (1999) Rietveld refinement guidelines. *J Appl Crystallogr* 32:36–50. <https://doi.org/10.1107/S0021889898009856>
- [46] Williamson GK, Hall WH (1953) X-ray line broadening from filed aluminium and wolfram. *Acta Metall* 1:22–31. [https://doi.org/10.1016/0001-6160\(53\)90006-6](https://doi.org/10.1016/0001-6160(53)90006-6)
- [47] Karolus M, Łągiewka E (2004) Crystallite size and lattice strain in nanocrystalline Ni–Mo alloys studied by Rietveld Refinement. *J Alloys Compd* 367:235–238. <https://doi.org/10.1016/j.jallcom.2003.08.044>
- [48] Karolus M (2006) Applications of Rietveld refinement in Fe-B-Nb alloy structure studies. *J Mater Process Technol* 175:246–250. <https://doi.org/10.1016/j.jmatprotec.2005.04.016>

- [49] Enjalbert R, Gally J (1986) A refinement of the structure of V_2O_5 . *J Acta Crystallogr C* 42:1467–1469. <https://doi.org/10.1107/S0108270186091825>
- [50] Kubelka P, Munk F (1931) Ein beitrage zur optik der farbanstriche. *Z Tech Phys* 12:593–601
- [51] Tauc J, Grigorovici R, Vancu A (1966) Optical properties and electronic structure of amorphous germanium. *Phys Status Solidi* 15:627–637. <https://doi.org/10.1002/pssb.19660150224>
- [52] Ramana CV, Smith RJ, Hussain OM (2003) Grain size effects on the optical characteristics of pulsed-laser deposited vanadium oxide thin films. *Phys Stat Sol A* 199:R4–R6. <https://doi.org/10.1002/pssa.200309009>
- [53] Masloboeva SM, Kadyrova GI, Kuznetsov VYa, Zalkind OA, Arutyunyan LG (2012) Synthesis and research of phase composition alloys $Nb_2O_5: Fe^{3+}$ and $Ta_2O_5: Fe^{3+}$. *Russ J Appl Chem* 85:1827–1831. <https://doi.org/10.1134/s1070427212120063>
- [54] Musić S, Popović S, Ristić M (1993) Chemical and structural properties of the system $Fe_2O_3-Cr_2O_3$. *J Mater Sci* 28:632–638. <https://doi.org/10.1007/BF01151237>
- [55] Botto IL, Vassallo MB, Baran EJ, Minelli G (1997) IR spectra of VO_2 and V_2O_3 . *Mater Chem Phys* 50:267–270. [https://doi.org/10.1016/S0254-0584\(97\)01940-8](https://doi.org/10.1016/S0254-0584(97)01940-8)
- [56] Ji H, Liu D, Cheng H, Zhang Ch, Yang L, Ren D (2017) Infrared thermochromic properties of monoclinic VO_2 nanopowders using a malic acid-assisted hydrothermal method for adaptive camouflage. *RSC Adv* 7:5189–5194. <https://doi.org/10.1039/C6RA26731A>
- [57] Birdeanu M, Birdeanu AV, Fagadar-Cosma E, Enache C, Miron I, Grozescu I (2013) Structural, morphological, optical and thermal properties of the $ZnTa_2O_6$ nanomaterials obtained by solid state method. *Dig J Nanomater Biostruct* 8:263–272
- [58] Husson E, Repelin Y, Brusset H (1980) Comparaison des champs de force des niobates, tantalates et antimonates de structure columbite et trirutile. *J Solid State Chem* 33:375–384. [https://doi.org/10.1016/0022-4596\(80\)90160-7](https://doi.org/10.1016/0022-4596(80)90160-7)
- [59] Husson H, Repelin Y, Brusset H, Cerez A (1979) Spectres de vibration et calcul du champ de force des antimonates et des tantalates de structure trirutile. *Spectrochim Acta* 35A:1177–1187. [https://doi.org/10.1016/0584-8539\(79\)80100-2](https://doi.org/10.1016/0584-8539(79)80100-2)
- [60] Repelin Y, Husson H, Brusset H (1981) Champ de force et caracterisation des liaisons dans les niobates et tantalates de structure de “blocs 1x2.” *J Solid State Chem* 37:328–334. [https://doi.org/10.1016/0022-4596\(81\)90495-3](https://doi.org/10.1016/0022-4596(81)90495-3)
- [61] Iordanova R, Dimitriev Y, Dimitriov V, Klissurski D (1994) Structure of $V_2O_5-MoO_3-Fe_2O_3$ glasses. *J Non-Cryst Solids* 167:74–80. [https://doi.org/10.1016/0022-3093\(94\)90369-7](https://doi.org/10.1016/0022-3093(94)90369-7)
- [62] Preudhomme J, Tarte P (1971) Infrared studies of spinels-III: The normal II–III spinels. *SpectrochimActa* 27A:1817–1835. [https://doi.org/10.1016/0584-8539\(71\)80235-0](https://doi.org/10.1016/0584-8539(71)80235-0)
- [63] Botto IL, Vassallo M, Munoz M, Cabello CI, Gambaro L (2009) $MVMoO_7$ substituted phases (M=Fe, Cr): structural stability, reducibility and catalytic properties in methanol oxidation. *J Arg Chem Soc* 97:250–265
- [64] Ghosh B, Dutta A, Brajesh K, Sinha TP (2015) Dielectric relaxion in double-perovskite Ca_2GdTaO_6 . *Indian J Pure Appl Phys* 53:125–133
- [65] Bayer G (1962) Isomorphie und morphotropibeziehungen bei oxyden mit TiO_2 -Typ und verwandten structuren. *Ber Deutsch Keram Ges* 39:535–554. <https://doi.org/10.3929/ethz-a-000089201>
- [66] Nabar MA, Phanasgaonkar DS (1983) Infrared spectral investigation of orthovanadates and CrO_6 groups in $TiM^{II}Cr_2(VO_4)_3$ compounds. *Spectrochim Acta* 39:777–779. [https://doi.org/10.1016/0584-8539\(83\)80016-6](https://doi.org/10.1016/0584-8539(83)80016-6)
- [67] Hanuza J, Hermanowicz K, Ogonowski W, Jeżowska-Trzebiatowska B (1983) The structure of the active V_2O_5/MgO catalyst layer on the basis of IR and Raman spectroscopic data. *Bull Pol Acad Sci Ser Sci Chim* 31:139–152
- [68] Iglesias JE, Ocaña M, Serna CJ (1990) Aggregation and matrix effects on the infrared spectrum of microcrystalline powders. *Appl Spectrosc* 44:418–426. <https://doi.org/10.1366/0003702904086227>

Publisher's Note Springer Nature remains neutral with regard to jurisdictional claims in published maps and institutional affiliations.